

Received August 2, 2020, accepted August 19, 2020, date of publication August 31, 2020, date of current version September 14, 2020.

Digital Object Identifier 10.1109/ACCESS.2020.3020374

Study of a Combined Surge Protective Device for a Relay Protection Circuit in a UHV Converter Station

YUQI ZHANG¹, WEIDONG ZHANG¹, AND JIANFEI JI²

¹State Key Laboratory of Alternate Electrical Power System With Renewable Energy Sources, North China Electric Power University, Beijing 102206, China

²Electric Power Research Institute, State Grid Jiangsu Electric Power Company, Nanjing 210036, China

Corresponding author: Yuqi Zhang (986953447@qq.com)

This work was supported by the State Grid Corporation of China through the Science and Technology Project under Grant 5226SX18000F.

ABSTRACT This article focuses on the problem that the voltage recovery time of relay protection circuits in converter stations is too long under lightning surges. A surge protective device (SPD) in a relay protection circuit in an ultrahigh-voltage (UHV) converter station is investigated. Based on the action characteristics of a gas discharge tube (GDT) and metal oxide varistor (MOV) under a $1.2/50 \mu\text{s}$ lightning surge, the equivalent circuit model of a series-combined SPD is established. In the equivalent circuit model, this study considers the breakdown voltage, nonlinear impedance, parasitic capacitance, stray inductance and other parameters of GDTs and MOVs. Simulation analysis shows that a series-combined SPD can significantly increase the residual voltage and shorten the voltage recovery time of the protected system. To verify the simulation results, a test platform based on a low-voltage DC voltage divider was built for the lightning surge test. The test results are consistent with the simulation results, verifying that a series-combined SPD can meet the dual surge protection requirements of peak suppression and fast voltage recovery.

INDEX TERMS Lightning surge protection, series-combined SPD, relay protection circuit, UHV converter station.

I. INTRODUCTION

The surge immunity test is an important test to evaluate the immunity of electrical and electronic equipment [1], [2], and it mainly simulates the unipolar surge caused by lightning and switching transient overvoltage. In the existing research, scholars have discussed the standard waveform [3] and mathematical form [4] of a lightning surge, the design method of the surge generator [5] and its applications [6]. Some scholars have pointed out that there is a lack of surge immunity test standards from the perspective of power line tests [7].

Regarding the research on surge suppression, the nonlinearity of the SPD volt-ampere characteristic has always been the focus of the equivalent circuit model [8]–[10]. In practical applications, the protection characteristics of SPDs are affected by many factors [11], [12]. For example, the input impedance of loads affects the effective protection distance of SPDs [13], and the increase in ground potential caused by lightning affects the residual voltage of low-voltage SPDs [14]. In addition, for the complex and harsh electromag-

netic environment of UHV transmission systems [15], [16], research on electromagnetic disturbance test methods [17], [18] and surge suppression measures [19], [20] has been carried out.

A DC voltage divider is an important device for voltage measurement in a UHVDC transmission system. Its measurement results directly affect the DC system control closed loop, which is closely related to the system reliability [21]. In September 2015, the voltage of a grounding grid in a ± 800 kV UHV converter station was raised due to a lightning strike, resulting in GDT breakdown for the DC voltage divider secondary surge protection and an instantaneous drop in the DC voltage in the relay protection circuit. Subsequently, the relay protection circuit voltage failed to recover to the normal value within 80 ms as requested, which caused DC undervoltage protection maloperation and DC blocking. This accident shows that the existing surge protection measures have defects and cannot meet the dual requirements of suppressing the surge peak value and quickly recovering voltage.

To solve this problem, experts at the China Electric Power Research Institute have put forward a series-combined SPD

The associate editor coordinating the review of this manuscript and approving it for publication was Dongbo Zhao.

composed of a GDT and MOV. Based on PSpice, this article establishes an equivalent circuit model for series-combined SPDs and studies the influence of the GDT and MOV parameters on the action characteristics of series-combined SPDs. The main contribution of this article is to verify that series-combined SPDs can effectively increase the residual voltage and shorten the voltage recovery time of the protected system of the relay protection circuit by means of simulation and testing.

II. EQUIVALENT CIRCUIT MODEL

A. BREAKDOWN CHARACTERISTICS OF A GDT

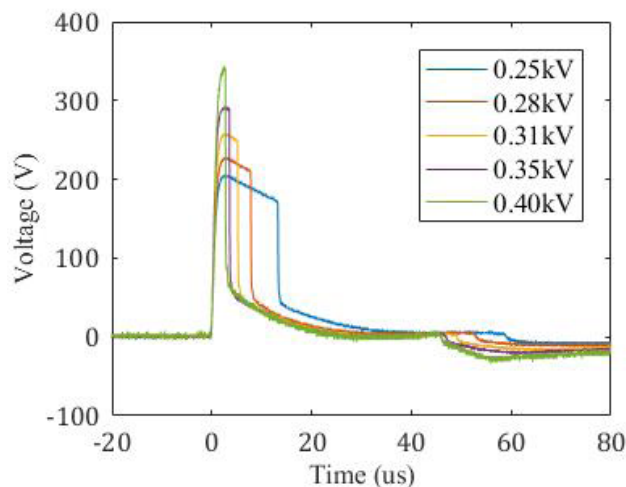
A GDT is a voltage-switching SPD. When the applied voltage increases so that the electric field strength between the poles exceeds the internal gas insulation strength, the gap discharges rapidly, and the voltage between the poles maintains a low residual voltage level. Under transient overvoltage, the breakdown speed of the gas gap depends on the development of the electron avalanche process. There is a delay in the gap discharge, and the actual breakdown voltage has some dispersion.

Switching operation and lightning transients are the causes of power system overvoltage. The IEC 61000-4-5 specifies the immunity requirements and test methods of unidirectional surges caused by overvoltage from switching and lightning transients. Considering the actual port type and overvoltage characteristics, a combination wave generator (1.2/50 μ s - 8/20 μ s) is selected as the excitation source in this article. The lightning surge generator used in the test can output a 1.2/50 μ s open-circuit voltage wave and an 8/20 μ s short-circuit current wave. By increasing the peak voltage of the lightning surge (V_{max}), the gradient of the applied voltage is increased. The breakdown characteristic curve of three GDTs under a lightning surge is recorded by an oscilloscope.

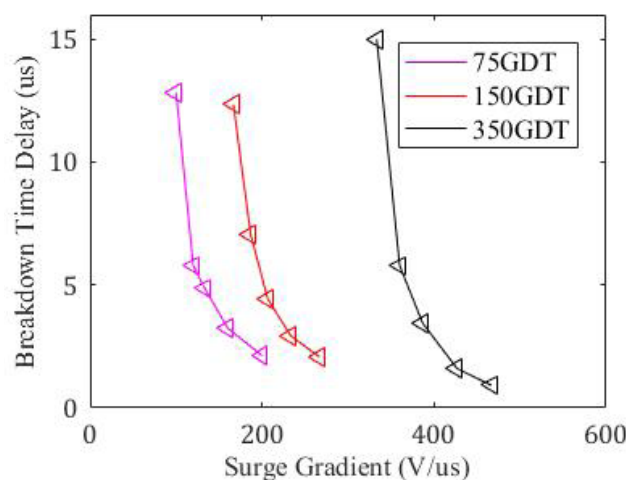
To study the influence of the surge gradient on the breakdown characteristics, three GDTs (75GDT, 150GDT and 350GDT) with different U_{fdc} are selected for testing. 75GDT refers to a gas discharge tube with a U_{fdc} of 75 V. The DC discharge voltage (U_{fdc}) of a GDT refers to the average value of the breakdown voltage under an overvoltage with a rising gradient lower than 100 V/s.

Fig. 1(a) shows the breakdown characteristic curve cluster for 150GDT under a lightning surge. The surge peak voltages corresponding to the five curves are 0.25 kV, 0.28 kV, 0.31 kV, 0.35 kV and 0.40 kV. The trend of the curve cluster shows that for the same gas discharge tube, the peak voltage of the lightning surge at the two poles significantly affects the breakdown delay and the actual breakdown voltage. With an increase in the surge voltage, the peak value of the transient pulse increases, and the breakdown delay decreases.

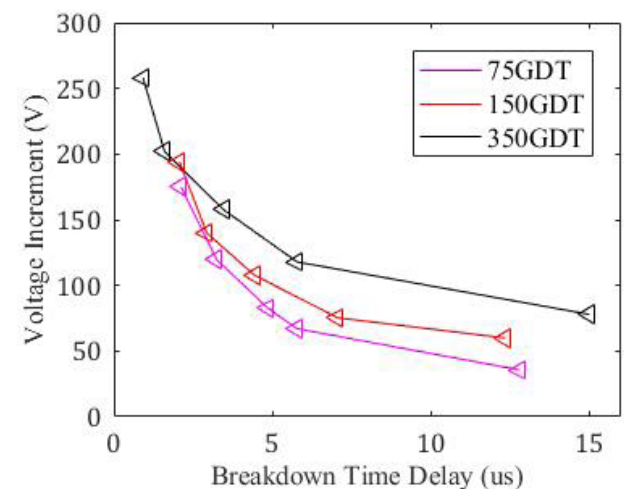
To analyze the breakdown characteristics of different GDTs, the waveform data recorded in the test are recorded in Table 1. The breakdown delay ($\Delta\tau$) of a GDT refers to the time interval between U_{fdc} and the actual breakdown voltage (U_{ft}). Table 1 reveals that the $\Delta\tau$ of a GDT is at the



(a)



(b)



(c)

FIGURE 1. Breakdown characteristic analysis of GDTs (a) 150GDT. (b) Relationship between the breakdown delay and surge gradient. (c) Relationship between the voltage increment and breakdown delay.

microsecond level (0.92-15 μ s) under a lightning surge. The surge gradient α and voltage increment ΔU are defined as

follows:

$$\alpha = \frac{0.8U_{max}}{1.2} \quad (1)$$

$$\Delta U = U_{ft} - U_{fdc} \quad (2)$$

As shown in Fig. 1(b), the breakdown delay decreases with increasing surge gradient. Under a surge gradient α of 200 V/ μ s, the breakdown delay of 75GDT is 2.12 μ s, and that of 150GDT is approximately 5 μ s. The comparison between the two data points shows that under the same surge gradient, a GDT with a higher U_{fdc} has a longer $\Delta\tau$. In addition, Fig. 1(c) shows the relationship between the voltage increment and the breakdown delay. Under a breakdown delay $\Delta\tau$ of 5.78 μ s, the voltage increment of 75GDT is 66.97 V, and that of 350GDT is 117.88 V, which indicates that a gas discharge tube with a higher U_{fdc} has a larger ΔU .

TABLE 1. Test waveform data of GDT breakdown characteristics.

GDT	$\Delta\tau$ (μ s)	α (V/ μ s)	ΔU (V)
75GDT	12.82	100	35.5
	5.78	120	66.97
	4.86	133.33	82.56
	3.24	160	119.56
	2.12	200	174.97
150GDT	12.35	166.67	29.91
	7.06	186.67	75.28
	4.42	206.67	107.91
	2.93	233.33	139.91
	2.07	266.67	193.94
350GDT	15	333.33	77.94
	5.78	360	117.88
	3.45	386.67	157.75
	1.6	426.67	201.94
	0.92	466.67	257.94

B. EQUIVALENT CIRCUIT MODEL OF A GDT

The breakdown characteristics of GDTs are affected by the waveform and gradient of the applied overvoltage, and most manufacturers do not provide a GDT model that can be used for simulation design. Therefore, this article establishes a GDT equivalent circuit suitable for a lightning surge. The equivalent circuit is based on previous research and incorporates the DC discharge voltage, actual breakdown voltage, breakdown delay and other parameters.

A schematic diagram of the equivalent circuit is shown in Fig. 2, which consists of three parts. R_v is the nonlinear resistance, which decreases with increasing applied voltage. The voltage-controlled switch is in the state of insulation resistance when it is turned off, and the resistance is zero when it is turned on. The signal voltage module is used to control whether the switch is on or off. When the input voltage exceeds the threshold voltage, the output voltage is high, and the voltage-controlled switch is turned on. When the input voltage decreases to less than 20 V, the output voltage changes from a high level to a low level, and the voltage-controlled switch is turned off.

Fig. 3 compares the simulation and test waveforms of the GDT breakdown characteristic. The fluctuation trend of the

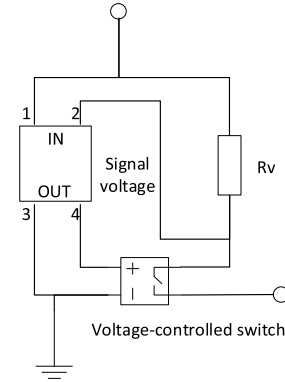


FIGURE 2. Schematic diagram of the GDT equivalent circuit.

two curves shows that the rising edge of the voltage wave is the same before the breakdown of the gas discharge tube. After the GDT breaks down, the simulation does not match well with the measurement in the wave tail. However, the accuracy of the wave tail is not important in this article. Therefore, the GDT model can be applied to the surge protection design under microsecond-level overvoltage.

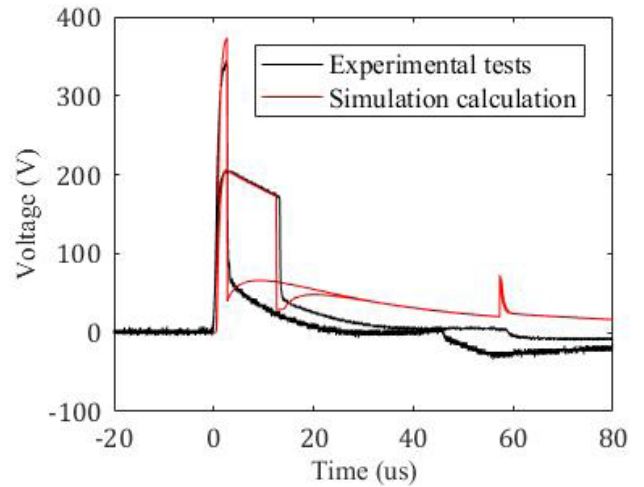


FIGURE 3. Comparison between the simulation and test waveforms of GDT breakdown characteristics.

C. EQUIVALENT CIRCUIT MODEL OF AN MOV

An MOV is a limited-voltage SPD with continuous volt-ampere characteristics. When the applied voltage is lower than the threshold voltage, the MOV has a high resistance. When the applied voltage is higher than the threshold voltage, the volt-ampere characteristic of the MOV shows high nonlinearity. Compared with the GDT, the MOV has a lower discharge capacity and a higher residual voltage. However, due to the large parasitic capacitance of the MOV, it will generate a large leakage current when applied in an AC system.

To meet the simulation requirements in the follow-up surge protection design, this article builds an equivalent circuit

model that can accurately simulate the MOV action characteristics under a $1.2/50 \mu\text{s}$ lightning surge. As shown in Fig. 4, the equivalent circuit consists of R_p , R_v , C and L . R_p represents the insulation state when the MOV is not in action in the equivalent circuit as a whole. The value of R_p will be of the hundreds of $M\Omega$. R_v is the nonlinear resistance when the applied voltage exceeds the threshold voltage. The nonlinear resistance (polynomial equation with several coefficients to be preset [10]) is replaced by only one diode in series with a controlled voltage source. C is the parasitic capacitance of hundreds to thousands of picofarads. L is the wiring inductance of approximately 1 nH/mm .

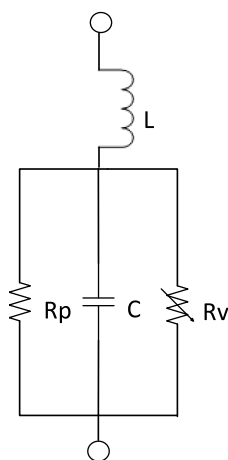


FIGURE 4. Equivalent circuit for the whole area.

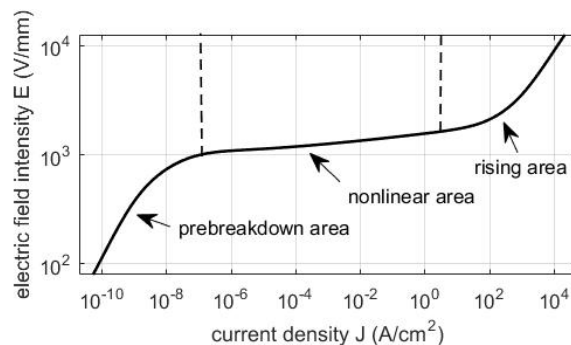
Fig. 5(a) shows the DC volt-ampere characteristics of the MOV. The curve can be divided into three sections: 1) the prebreakdown area, 2) the nonlinear area, and 3) the rising area. The volt-ampere characteristic of the prebreakdown area is linear. When the applied voltage is higher than the threshold voltage, the MOV enters the nonlinear region, in which a small increase in voltage will cause the current to increase by several orders of magnitude. Finally, the volt-ampere characteristic tends to be linear again, but the voltage rising speed in the rising area is much faster than that in the prebreakdown area.

The breakdown voltage of the MOV (U_{1mA}) refers to the voltage when passing a 1 mA DC current on the MOV. 100MOV refers to a metal oxide varistor with a U_{1mA} of 100 V . In Fig. 5(b), the simulation and test waveforms of 100MOV under a $1.2/50 \mu\text{s}$ lightning surge are compared. From the peak values and attenuation trends of the two curves, the equivalent circuit model reflects the action characteristics of the actual MOV.

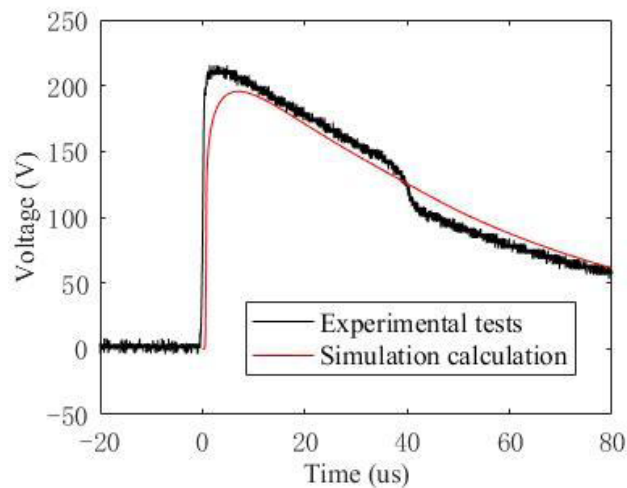
III. SERIES-COMBINED SPD

A. PARAMETER ANALYSIS OF A SERIES-COMBINED SPD

It can be seen from the study of GDT breakdown characteristics that a GDT can effectively reduce the peak value of transient overvoltage. However, the residual voltage is too low, and the voltage recovery time is too long after GDT



(a)



(b)

FIGURE 5. (a) DC volt-ampere characteristics of the MOV. (b) Comparison between the simulation and test waveforms of the MOV action characteristics.

breakdown. Compared with the protection measure of using a GDT alone, connecting an MOV in series can increase the residual voltage of the protected system after the series-combined SPD action. Meanwhile, the MOV in series can block the continuous current of the GDT to make it turn off. Therefore, a series-combined SPD can effectively suppress a surge and recover the working voltage of the protected system within 80 ms , which can meet the dual requirements on the surge protection characteristics in the actual project.

The series-combined SPD in Fig. 6(a) is composed of an MOV and GDT, which have different action characteristics. In the test, different types of MOVs and GDTs are selected for series combination. The voltage waveform of a 50Ω resistance is recorded after the series-combined SPD action, and influence of parameters U_{1mA} and U_{fdc} on the action characteristics of the series-combined SPD are analyzed. As shown in Fig. 6(b), a series-combined SPD action characteristic test system is built.

To eliminate the influence of different batch factors on the test, the same types of MOVs and GDTs are selected in each batch. In the test, three types of GDT are selected with different U_{fdc} parameters, from 150 to 600 V , and three types of MOV, with U_{1mA} parameters from 33 to 100 V , which are

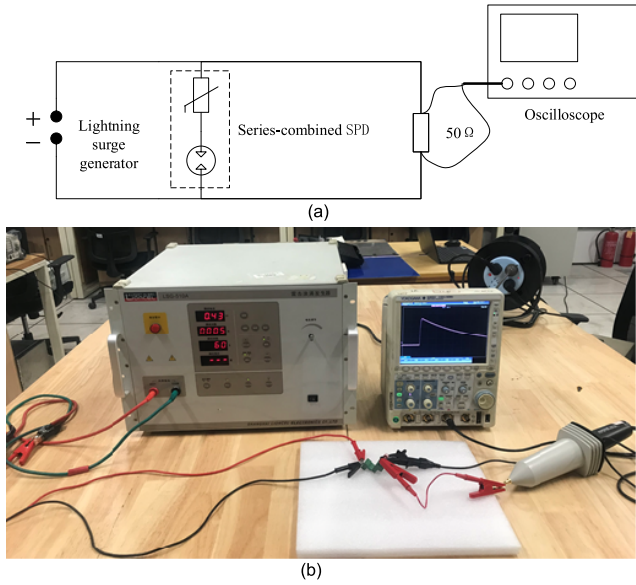


FIGURE 6. Test system of series-combined SPD action characteristics. (a) Schematic diagram. (b) Actual wiring diagram.

divided into two groups to carry out the test. The oscilloscope is set as a single-pulse rising-edge trigger. Under a lightning surge, the voltage waveform of 50 Ω resistance is recorded.

Fig. 7(a) reveals that under the same surge, the U_{fdc} of the GDT will affect the U_{ft} of the series-combined SPD, which is positively correlated with it. In Fig. 7(b), the residual voltage of the 50 Ω resistance increases with increasing U_{1mA} . From the perspective of overvoltage suppression, the smaller the instantaneous pulse peak value between U_{fdc} and U_{ft} under the same surge is, the better the overvoltage suppression performance of the SPD. From the perspective of shortening the voltage recovery time, properly increasing the residual voltage is conducive to the rapid recovery of the system working voltage. Therefore, when using a series-combined SPD, the MOV and GDT should be selected according to the surge protection characteristics.

B. PARAMETER SELECTION FOR A SERIES-COMBINED SPD

In the design of surge protection circuits, the selection of GDTs should adopt an empirical method. The parameters can be selected according to the operating conditions of GDTs in the protected system. For an AC system, GDTs should be able to ensure that no maloperation occurs within the normal operating voltage range and allowable fluctuation range of the line. Therefore, U_{fdc} should meet the following requirements:

$$\min(U_{fdc}) \geq 1.25 \times 1.15U_p \quad (3)$$

Here, U_{fdc} is the DC discharge voltage; U_p is the peak value of the normal operating voltage of the line; 1.15 is the maximum allowable fluctuation of the system operating voltage; and 1.25 is the additional 25% safety margin.

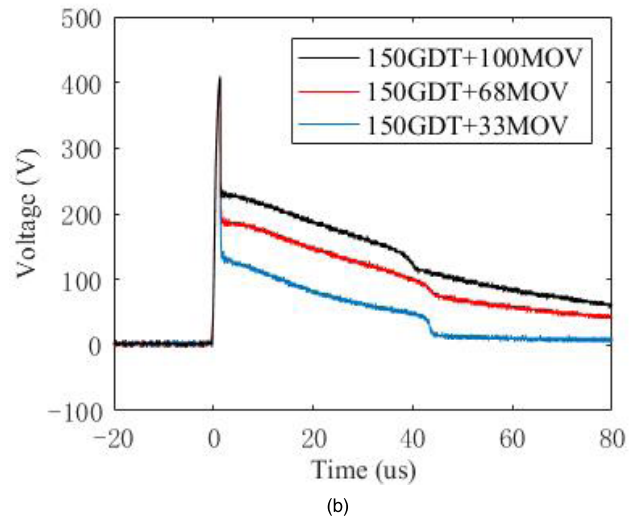
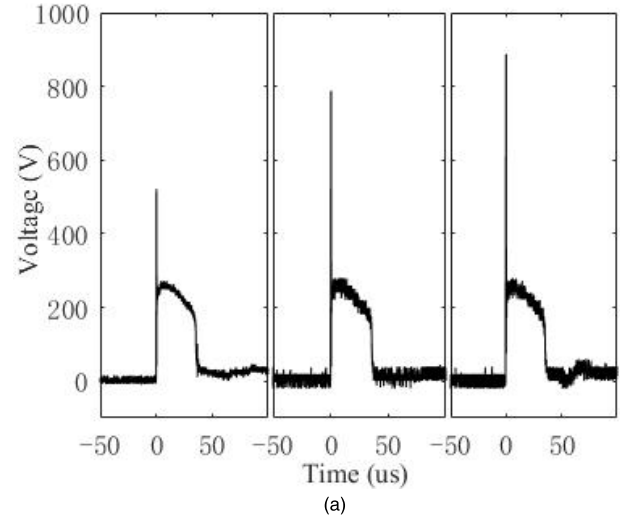


FIGURE 7. Analysis of the action characteristics of a series-combined SPD. (a) The influence of GDT parameters on a series-combined SPD. (b) The influence of MOV parameters on a series-combined SPD.

If the allowable deviation of U_{fdc} is 0.2, then

$$\min(U_{fdc}) = (1 - 0.2)U_{fdc} \quad (4)$$

Eq. (5) can be obtained by combining (3) and (4):

$$U_{fdc} \geq \frac{1.25 \times 1.15}{0.8}U_p \approx 1.8U_p \quad (5)$$

Similarly, for a GDT in a DC system,

$$U_{fdc} = 1.8U_{DC} \quad (6)$$

To reduce the possibility of series-combined SPD maloperation, the U_{fdc} of a GDT should be large. However, the U_{fdc} parameter affects the U_{ft} of the series-combined SPD, so it may exceed the withstand value of the protected system and damage the equipment. Therefore, the characteristics of the GDT should be considered in the trade-off between the two requirements.

The MOV should be selected to block the continuous current (0.1-0.4 A) in the arc area of the GDT. Considering that the voltage of a GDT in the arc area is generally approximately 20 V and the normal operating voltage at the secondary side of the DC voltage divider is 70 V, a reasonable option can be chosen. When the voltage of the MOV is 50 V, the current should be less than the continuous current of the GDT arc area, which can be conservatively taken as 50 mA.

IV. SURGE PROTECTION MEASURES FOR THE SECONDARY SIDE OF A DC VOLTAGE DIVIDER

A. TRANSIENT CHARACTERISTIC ANALYSIS OF A DC VOLTAGE DIVIDER

An 800 kV converter station reduces the 800 kV DC voltage to 70 V through a DC voltage divider and introduces it into the balance module. The balance module is then transmitted to the secondary circuit through an isolation amplifier. To analyze the transient characteristics of voltage recovery at the secondary side of the DC voltage divider, the equivalent circuit of the DC voltage divider is established, as shown in Fig. 8. This equivalent circuit is based on the actual parameters of the DC voltage divider in the converter station.

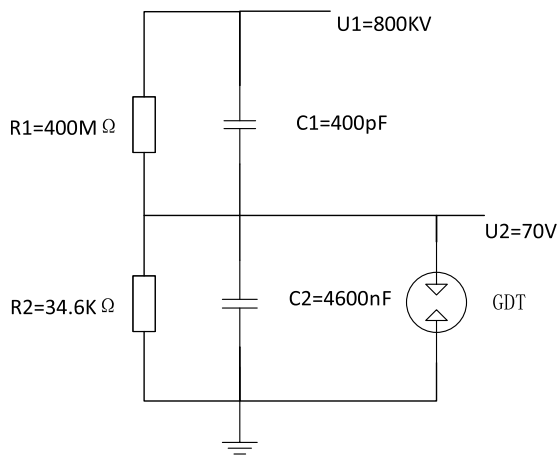


FIGURE 8. Equivalent circuit of the DC voltage divider.

By analyzing the equivalent circuit of the DC voltage divider, the differential voltage equation between U_2 and U_1 can be obtained:

$$C_1 \frac{du_1}{dt} + \frac{u_1}{R_1} = (C_1 + C_2) \frac{du_2}{dt} + \left(\frac{R_1 + R_2}{R_1 R_2}\right) u_2 \quad (7)$$

After the GDT breaks down, the initial value of U_2 is 0 V, but the initial value of U_1 is $V_D = 800$ kV. In the process of secondary-side voltage recovery, U_1 remains unchanged, so the U_2 voltage recovery equation can be derived as

$$U_2(t) = \frac{R_2 V_D}{R_1 + R_2} \left[1 - e^{-\frac{R_1 + R_2}{R_1 R_2 (C_1 + C_2)} t} \right] \quad (8)$$

It can be seen from (8) that the capacitance C_2 is limited, and the voltage U_2 cannot be changed suddenly; $U_{2(0+)} = 0$ V. With C_2 charging, U_2 gradually changes to the steady-state

value:

$$U_2(\infty) = \frac{R_2 V_D}{R_1 + R_2} \quad (9)$$

Therefore, the time constant τ of the secondary-side voltage recovery process can be obtained:

$$\tau = \frac{R_1 R_2 (C_1 + C_2)}{R_1 + R_2} = 159ms \quad (10)$$

After the GDT breaks down instantaneously, the secondary voltage of the DC voltage divider must undergo a transient process of hundreds of milliseconds before it can return to the normal operating voltage.

B. SIMULATION ANALYSIS OF A DC VOLTAGE DIVIDER

The simulation circuit of the DC voltage divider is shown in Fig. 9, and it can be divided into three parts. The first part is the DC voltage divider circuit, which is composed of V1, R1, R2, C1 and C2. The second part is the 1.2/50 μs lightning surge generator circuit, which is composed of the capacitor C_{s1} and the resistance and inductance elements forming the rising edge. The third part is the GDT circuit model, which is primarily composed of a voltage-controlled switch, the nonlinear controlled source and a signal voltage module.

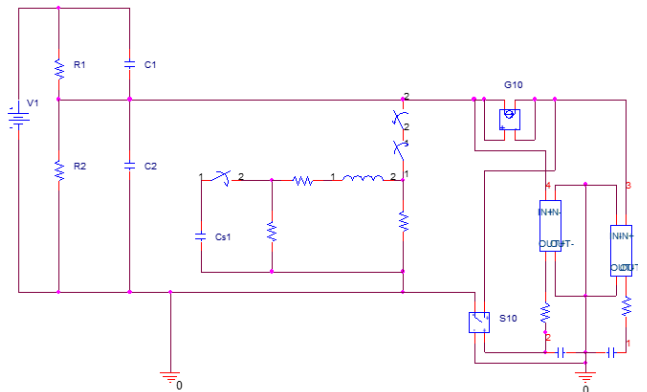


FIGURE 9. Simulation circuit of the DC voltage divider.

When a lightning surge is applied to the secondary side of the voltage divider, the measured voltage of C_2 is as shown in Fig. 10(a). The simulation results show that the voltage of C_2 drops to 20.4 V after the GDT breaks down. The voltage of C_2 then rises slowly and reaches 70 V after nearly 500 ms, which cannot meet the requirement (80 ms) of DC undervoltage protection. Therefore, it is necessary to increase the existing surge protection measures to shorten the voltage recovery time.

In previous research, it has been verified that the series-combined SPD has a high residual voltage. A high residual voltage means a reduction in the voltage recovery time. In Fig. 10(b), the protection effects of different series-combined SPDs are compared. The voltage recovery time with the series-combined SPD protection is significantly shorter than

that with the GDT alone. The residual voltage increases with increasing U_{1mA} . In all combinations, 150GDT and 66MOV in series have the best voltage recovery effect, and the voltage can be recovered to 70 V within 80 ms.

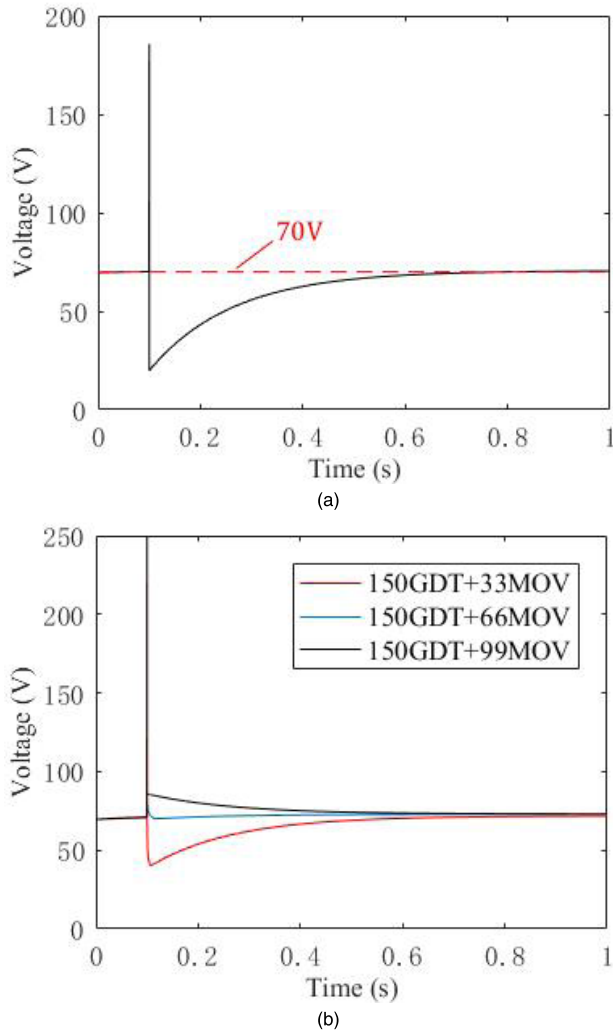


FIGURE 10. Voltage recovery of C2 on the secondary side after a lightning strike (a) with 150GDT; (b) with a series-combined SPD.

C. LIGHTNING SURGE TEST BASED ON A LOW-VOLTAGE DC VOLTAGE DIVIDER

The simulation results show that a series-combined SPD can effectively increase the residual voltage and shorten the voltage recovery time of the protected system. To verify the correctness of this conclusion, a lightning surge test platform is constructed based on a low-voltage DC voltage divider. The lightning surge generator selected in the test is LSG-510A. Its open-circuit voltage wave front edge is $1.2 \pm 30\% \mu s$, its pulse width is $50 \pm 20\% \mu s$, and its peak value is 0-10 kV. The DC voltage source selected is DH1722. Its output voltage is 0-250 V, and its output current is 0-1.2 A. The U_{1mA} of the MOV ranges from 22 to 100 V, and the U_{fdc} of the GDT is 150 V in the test.

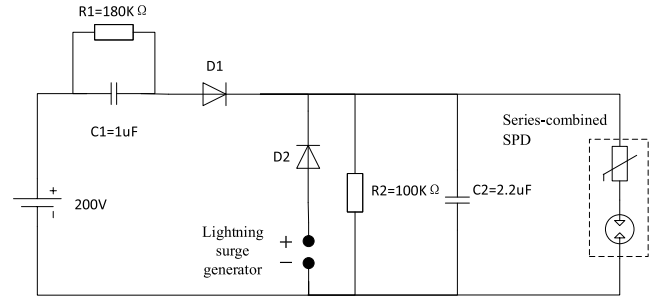


FIGURE 11. Lightning surge test circuit based on a low-voltage DC voltage divider.

The test circuit is shown in Fig. 11. In this circuit, R1, C1, R2 and C2 simulate the high- and low-voltage bridge arms of the DC voltage divider. The function of diode D1 is to prevent the DC voltage source from being burned out by a lightning surge counterattack. The function of diode D2 is to keep the surge generator disconnected from the external circuit when it is not working. In the test, different types of MOVs and GDTs are selected in series. The C2 voltage recovery characteristics under a $1.2/50 \mu s$ lightning surge are tested, and the results are shown in Table 2.

TABLE 2. Voltage recovery characteristics of different series-combined SPDs.

SPD	U_{fde} (V)	Voltage at 80 ms (V)	U_{fl} (V)
150GDT	70DC	40	238
150GDT+22MOV	70DC	55	80
150GDT+33MOV	70DC	60	102
150GDT+56MOV	70DC	72	138
150GDT+68MOV	70DC	80	168
150GDT+100MOV	70DC	82	293

Table 2 reveals that the selection of different MOVs will lead to different voltage recovery effects. The voltage recovery effect is best when 56MOV and 150GDT are used in series. In 80 ms, the voltage can recover to 72 V, which meets the requirement of DC undervoltage protection. The comparison of the voltage recovery characteristics of different series-combined SPDs is shown in Fig. 12.

By comparing the test waveform in Fig. 12 with the simulation waveform in Fig. 10, it can be seen that the test and simulation results are consistent. When the GDT is used alone as the surge protection device, the voltage recovery time is approximately 500 ms. After using a series-combined SPD as the surge protection device, the voltage recovery time can be shortened to within 80 ms, which can prevent the maloperation of DC undervoltage protection and meet the needs of the actual project.

V. CONCLUSION

Based on a $1.2/50 \mu s$ lightning surge test, this article presents the equivalent circuit model of a GDT and MOV in PSpice.

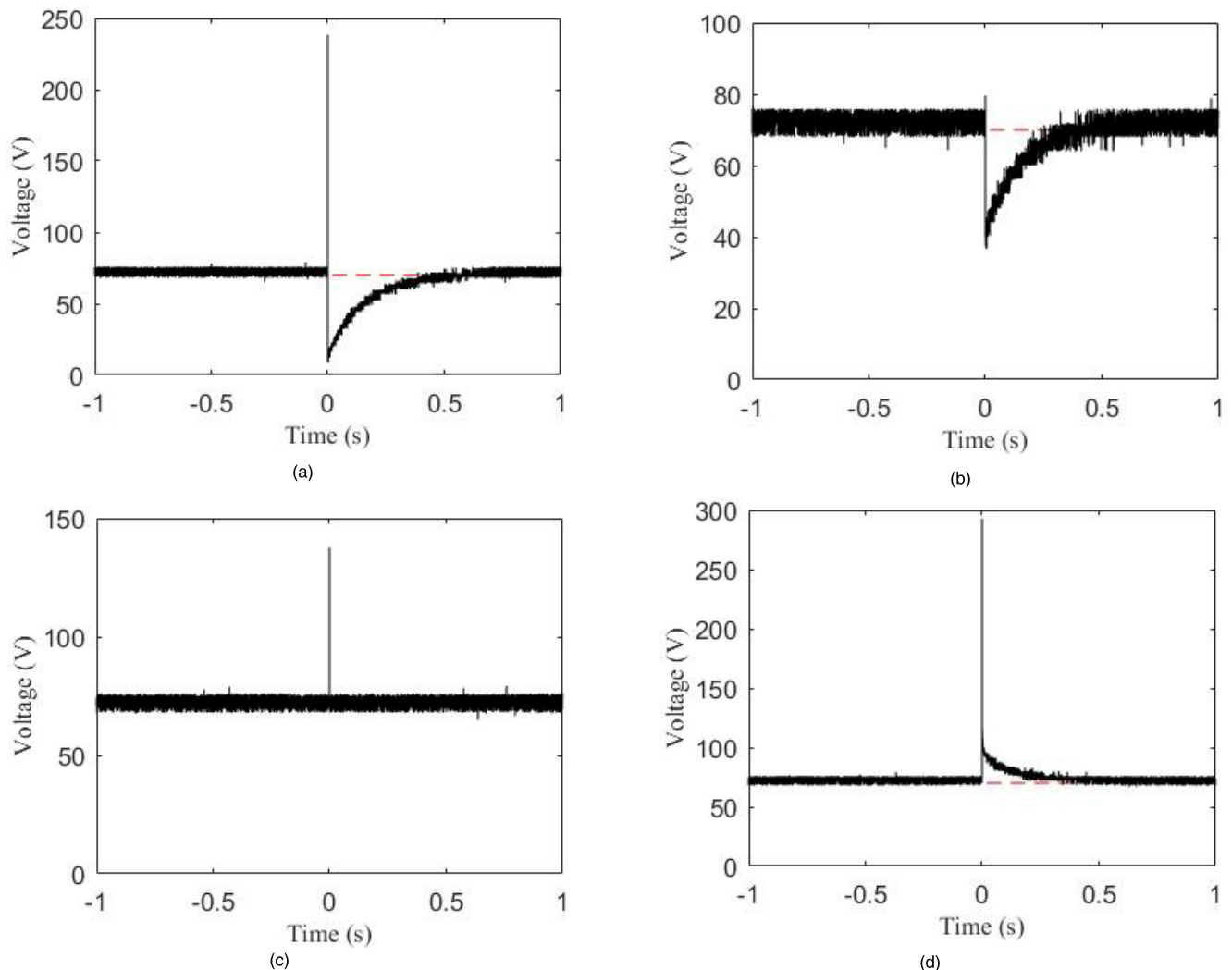


FIGURE 12. Voltage recovery of C2 (a) with 150GDT; (b) with 150GDT+22MOV; (c) with 150GDT+56MOV; (d) with 150GDT+100MOV.

By comparing the simulation and test waveforms, the applicability of the equivalent circuit model in microsecond-level surge protection design is verified.

The influence of the GDT and MOV parameters on the series-combined SPD is analyzed by simulations and tests, and the parameter selection method for the series-combined SPD is described.

Finally, a lightning surge test based on a low-voltage DC voltage divider is carried out. The test results show that the application of the series-combined SPD can significantly shorten the recovery time of the protected system and meet the requirement of DC undervoltage protection in practical engineering. The research content of this article can provide a reference for the design of surge protection in similar relay protection circuits with dual requirements.

REFERENCES

- [1] *Electromagnetic Compatibility (EMC)—Part 4-5: Testing and Measurement Techniques—Surge Immunity Test*, Standard 61000-4-5, 2017.
- [2] *Low-Voltage Surge Protective Devices—Part 11: Surge Protective Devices Connected to Low-Voltage Power Systems—Requirements and Test Methods*, Standard 61643-11, 2011.
- [3] S. Okabe, J. Takami, T. Tsuboi, G. Ueta, A. Ametani, and K. Hidaka, "Discussion on standard waveform in the lightning impulse voltage test," *IEEE Trans. Dielectr. Electr. Insul.*, vol. 20, no. 1, pp. 147–156, Feb. 2013.
- [4] T.-C. Toh, "A mathematical formalism for surge generator correlation," *IEEE Trans. Electromagn. Compat.*, vol. 53, no. 2, pp. 547–551, May 2011.
- [5] J. Birkl and P. Zahlmann, "Extremely high lightning currents a newly designed surge generator and some practical applications," in *Proc. Int. Conf. Lightning Protection (ICLP)*, Oct. 2014, pp. 1183–1188.
- [6] C. F. M. Carobbi and A. Bonci, "Elementary and ideal equivalent circuit model of the 1, 2/50-8/20 μ s combination wave generator," *IEEE Electromagn. Compat. Mag.*, vol. 2, no. 4, pp. 51–57, 2013.
- [7] M. Zhou, H. Zhang, L. Cai, X. Fan, J. Wang, S. Dai, and J. Xue, "Surge immunity test of personal computer at power lines," in *Proc. 7th Asia-Pacific Int. Conf. Lightning*, Nov. 2011, pp. 813–816.
- [8] J. G. Zola, "Gas discharge tube modeling with PSpice," *IEEE Trans. Electromagn. Compat.*, vol. 50, no. 4, pp. 1022–1025, Nov. 2008.
- [9] A. Larsson, V. Scuka, K. Borgeest, and J. Luiken ter Haseborg, "Numerical simulation of gas discharge protectors—A review," *IEEE Trans. Power Del.*, vol. 14, no. 2, pp. 405–410, Apr. 1999.
- [10] J. G. Zola, "Simple model of metal oxide varistor for pspice simulation," *IEEE Trans. Comput.-Aided Design Integr. Circuits Syst.*, vol. 23, no. 10, pp. 1491–1494, Oct. 2004.

- [11] Z. He and Y. Du, "SPD protection distances to household appliances connected in parallel," *IEEE Trans. Electromagn. Compat.*, vol. 56, no. 6, pp. 1377–1385, Dec. 2014.
- [12] J. He, Z. Yuan, S. Wang, J. Hu, S. Chen, and R. Zeng, "Effective protection distances of low-voltage SPD with different voltage protection levels," *IEEE Trans. Power Del.*, vol. 25, no. 1, pp. 187–195, Jan. 2010.
- [13] J. He, Z. Yuan, J. Xu, S. Chen, J. Zou, and R. Zeng, "Evaluation of the effective protection distance of low-voltage SPD to equipment," *IEEE Trans. Power Del.*, vol. 20, no. 1, pp. 123–130, Jan. 2005.
- [14] S. Chen, Y. Zhang, C. Chen, X. Yan, W. Lu, and Y. Zhang, "Influence of the ground potential rise on the residual voltage of low-voltage surge protective devices due to nearby lightning flashes," *IEEE Trans. Power Del.*, vol. 31, no. 2, pp. 596–604, Apr. 2016.
- [15] S. Okabe, M. Kan, and T. Kouno, "Analysis of surges measured at 550 kV substations," *IEEE Trans. Power Del.*, vol. 6, no. 4, pp. 1462–1468, Oct. 1991.
- [16] F. O. Resende and J. A. Peças Lopes, "Using low-voltage surge protection devices for lightning protection of 15/0.4 kV pole-mounted distribution transformer," *CIREN Open Access Proc. J.*, vol. 2017, no. 1, pp. 888–892, Oct. 2017.
- [17] W. Shipu, P. Wenlong, Y. Zhining, Z. Kejie, and W. Xixiu, "Study on the reliability of new kind of ± 1 100 kv DC voltage divider under the action of impulse voltage," *J. Eng.*, vol. 2019, no. 16, pp. 2575–2579, Mar. 2019.
- [18] X. Chen, C. Xia, W. Shi, T. Lu, T. Lei, and X. Zhao, "Study on direct lightning protection of ± 1100 kV converter station grid," in *Proc. 11th Asia-Pacific Int. Conf. Lightning (APL)*, Jun. 2019, pp. 1–5.
- [19] M. Broker and V. Hinrichsen, "Testing Metal-Oxide varistors for HVDC breaker application," *IEEE Trans. Power Del.*, vol. 34, no. 1, pp. 346–352, Feb. 2019.
- [20] X. Zhang, W. Zhang, B. Xu, and J. Zhang, "Research on conducted and radiated electromagnetic interference of VSC-HVDC transmission system," in *Proc. IEEE Int. Symp. Electromagn. Compat. IEEE Asia-Pacific Symp. Electromagn. Compat. (EMC/APEMC)*, May 2018, p. 29.
- [21] J. Zhang, T. Lu, W. Zhang, J. Xu, and W. Li, "Measurement and analysis of radiated disturbance characteristics of ± 320 kV modular multilevel converter system," *IEEE Access*, vol. 7, pp. 10028–10036, 2019.



YUQI ZHANG was born in Yichun, China, in 1996. He is currently pursuing the M.Sc. degree in electrical engineering with North China Electric Power University, Beijing, China.

His main research interests include electromagnetic environments and electromagnetic compatibility in electric power systems.



WEIDONG ZHANG was born in Baoding, China, in 1967. He received the B.Sc. degree in electromagnetic field and microwave technology from the Beijing Broadcasting Institute, Beijing, China, in 1990, and the M.Sc. and Ph.D. degrees in electrical engineering from North China Electric Power University, Baoding, in 1996 and 2003, respectively.

He is currently a Professor with the School of Electrical and Electronic Engineering, North China Electric Power University. His research interests include electromagnetic environments and electromagnetic compatibility in electric power systems, and transient measurement techniques in various applications.

JIANFEI JI, photograph and biography not available at the time of publication.

• • •